Environmental Science & Technology

Article

pubs.acs.org/est

Deposition and Survival of *Escherichia coli* O157:H7 on Clay Minerals in a Parallel Plate Flow System

Peng Cai,[†] Qiaoyun Huang,[†] and Sharon L. Walker*[,‡]

[†]State Key Laboratory of Agricultural Microbiology, Huazhong Agricultural University, Wuhan 430070, China

[‡]Department of Chemical and Environmental Engineering, University of California, Riverside, California 92521, United States

Supporting Information

ABSTRACT: Understanding bacterial pathogens deposition and survival processes in the soil−groundwater system is crucial to protect public health from soilborne and waterborne diseases. However, mechanisms of bacterial pathogen−clay interactions are not well studied, particularly in dynamic systems. Also, little is known about the viability of bacterial pathogens when attached to clays. In this study, a parallel plate flow system was used to determine the deposition kinetics and survival of *Escherichia coli* O157:H7 on montmorillonite, kaolinite, and goethite over a wide range of ionic strengths (IS) (0.1−100 mM KCl). *E. coli* O157:H7 deposition on the positively charged goethite is greater than that on the negatively charged kaolinite and montmorillonite. Although the zeta potential of kaolinite was more negative than that of montmorillonite, kaolinite showed a greater deposition for *E. coli* O157:H7 than montmorillonite, which is attributed to the chemical heterogeneity of clay minerals. Overall, increasing IS resulted in an increase of *E. coli* O157:H7 deposition on montmorillonite and kaolinite, and a decrease on goethite. Interaction energy calculations suggest that *E. coli* O157:H7 deposition on clays was largely governed by DLVO (Derjaguin−Landau−Verwey−Overbeek) forces. The loss of bacterial membrane integrity was investigated as a function of time using the Live/Dead BacLight viability assay. During the examined period of 6 h, *E. coli* O157:H7 retained its viability in suspension and when attached to montmorillonite and kaolinite; however, interaction with the goethite was detrimental. The information obtained in this study is of fundamental significance for the understanding of the fate of bacterial pathogens in soil environments.

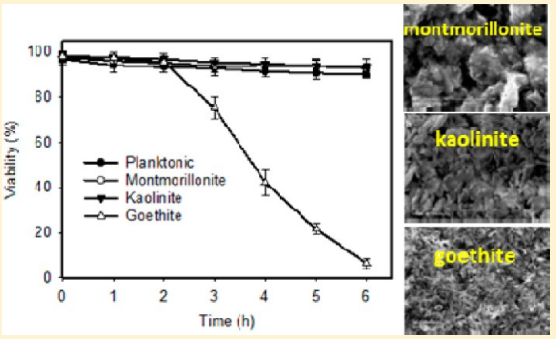

INTRODUCTION

Enterohemorrhagic *Escherichia coli* O157:H7, a Gram-negative pathogenic bacterium, can cause severe gastrointestinal disease, such as diarrhea and hemolytic uremic syndrome in humans.[1] It was reported that *E. coli* O157:H7 causes 73,480 illnesses, 2,168 hospitalizations, and 61 deaths each year in the United States.[2] Outbreaks of *E. coli* O157: H7 infections in humans are always traced back to contact with contaminated food, soil, surface or groundwater.[3,4] Therefore, a thorough understanding of the fate of *E. coli* O157:H7 in the subsurface environments is of great importance and can be used to assess and mitigate the potential risk to public health.

E. coli O157:H7 deposition (the process of particle transport and interaction with a surface) in saturated porous media has been reported in recent years as a function of solid surface characteristics, solution chemistry, and extracellular macromolecules.[5−12] For example, Morrow et al.[5] reported that in macroscale column experiments pyrophyllite and Pyrax (a composite form of pyrophyllite, mica, and silica) showed significantly higher bacterial retention, larger deposition coefficients, and lower initial cell breakthrough values for *E. coli* O157:H7 than did α-alumina, silica, or dolomite. Kim et al.[9] reported that *E. coli* O157:H7 deposition on quartz sand was inversely proportional to ionic strength (IS) (1−100 mM) at higher pH conditions (8.4 and 9.2), whereas no effect of IS was observed at pH 5.8. These trends cannot be explained by classic DLVO theory, which accounts only for electrostatic and van der Waals interactions. An additional non-DLVO type interaction, electrosteric repulsion, occurred at high IS ($\geq$ 10 mM) due to the presence of extracellular macromolecules that hindered *E. coli* O157:H7 adhesion to the quartz surface.[10] Wang et al.[11] found that phosphate could enhance the transport of *E. coli* O157:H7 cells under IS 10 and 100 mM and increased phosphate in the mobile aqueous phase led to the release of previously immobilized *E. coli* O157:H7 cells. However, these studies focused on bacteria transport in the column packed with primary minerals. In reality, surfaces exposed to bacteria in soils and sediments include primary minerals, clay minerals, and organic matter.

Clay minerals are the most active inorganic colloid components in soils and sediments.[13] Due to their surface electrical properties, clay minerals have been widely used to remove heavy metals and organic pollutants. Adsorption of

Received: November 16, 2012
Revised: January 22, 2013
Accepted: January 24, 2013
Published: January 24, 2013

ACS Publications © 2013 American Chemical Society

dx.doi.org/10.1021/es304686a | Environ. Sci. Technol. 2013, 47, 1896−1903

bacteria on clay minerals has also been investigated recently.[13−19] For example, *Pseudomonas putida* preferred to adsorb on the surface of goethite, followed by kaolinite and montmorillonite.[13] Electrostatic interactions and hydrogen bonding were mainly considered to contribute to the adsorption of *P. putida* on montmorillonite, kaolinite, and goethite.[14,15] Attenuated total reflectance (ATR) Fourier transform infrared (FTIR) spectroscopy revealed significant short-range bonding interactions (P−OFe bond formation) occur upon adhesion of *Shewanella oneidensis*, *Pseudomonas aeruginosa*, and *Bacillus subtilis* cells to the positively charged hematite surface at pH 7.1.[16] The inner-sphere attachment mode of phosphate groups from bacteria or their extracellular polymeric substances (EPS) on iron oxides varies with pH.[17,18] In the reactions of *P. putida* EPS with goethite, inner-sphere complexes (Fe−phosphate) types changed from monodentate to bidentate with increasing pH from 3.0 to 9.0.[18] Isothermal titration calorimetry (ITC) demonstrated that electrostatic force may play a more important role in the *B. subtilis* adsorption on goethite than that on phyllosilicates (montmorillonite and kaolinite).[19] However, the above bacterial adsorption studies with clay minerals were conducted in batch systems, which do not consider mass transport processes and do not necessarily reproduce the dynamic reaction conditions taking place in the real environment. To our knowledge, deposition of *E. coli* O157:H7 on clay surfaces in a continuous flow mode has never been explored.

Studies on *E. coli* O157:H7 survival in the subsurface environments showed that *E. coli* O157:H7 can persist in bovine feces for an extended period time.[20−28] For example, Jiang et al.[21] reported that *E. coli* O157:H7 survived for up to 77, >226, and 231 days in manure-amended autoclaved soil held at 5, 15, and 21 °C, respectively. Semenov et al.[22] presented that *E. coli* O157:H7 survived in soils treated with inoculated manure or slurry for 17.1 and 27.6 days, respectively. Avery et al.[23] reported that *E. coli* O157:H7 in lake and river water microcosms kept at 10 °C with an initial concentration of 10^5 cells/mL were viable after 2 months at a concentration of 10 cells/mL. The Weibull model was constructed based on the hypothesis that the population is composed of two subpopulations differing in their capability to resist the stresses, and deactivation kinetics of both subpopulations follows a Weibull distribution.[24] The Weibull model has also been used for calculating T_d (time needed to reach the detection limit). In one particular study, this model was applied and the calculated T_d (time needed to reach the detection limit of 100 CFU/g soil in this case) for *E. coli* O157:H7 in loamy sand, sandy loam, and silty clay was 32, 80, and 110 days, respectively.[25] The authors also found T_d was positively correlated with soil structure (e.g., clay content) and soil chemistry (e.g., total nitrogen, total carbon, and water extractable organic carbon). These studies clearly indicate that *E. coli* O157:H7 has the potential to survive a substantial amount of time in various aquatic and soil environments; however, there remains a dearth of knowledge on bacterial survival in clayey soil which contains more than 50% of clay minerals.[26]

A few studies have examined the viability of cells on different biomaterial surfaces in a parallel plate flow chamber using the Live/Dead viability kit.[29−32] For example, van der Mei et al.[30] reported that polydiallyldimethylammonium chloride (p-DADMAC) coatings on glass enhanced adhesion and reduced the viability of selected bacteria by the positively charged ammonium groups. Compared to basic wood-based carbon and coconut-based carbon, the number of *Raoultella terrigena* and *E. coli* adhesion to the acidic wood-based carbon was the highest and caused the greatest loss of viability.[31] Recently, Asadishad et al.[32] demonstrated Live/Dead BacLight staining technique was sensitive enough to distinguish between the loss of viability kinetics of different bacteria attached to various surfaces. They also found that the viability of bacteria attached to positively charged 3-aminopropyltriethoxysilane (APTES)-coated glass decreased significantly over time compared with bare glass. However, there is no study on the effect adhesion to clay surfaces has on bacterial viability.

This study was designed to address these two gaps in the literature, to investigate the deposition and survival kinetics of *E. coli* O157:H7 on montmorillonite, kaolinite, and goethite in a dynamic, parallel plate flow system. The advantages of this system are as follows: (i) it allows bacteria−clay interactions to occur under controlled mass transport conditions and (ii) attached bacterial viability can be determined in situ and real-time. To achieve this purpose, both the deposition kinetics and viability of cells were quantified on glass surfaces coated with three representative clay minerals. Additionally, surface properties of *E. coli* O157:H7 and the clay surfaces were extensively characterized.

MATERIALS AND METHODS

Bacterial Cell Preparation and Characterization. *E. coli* O157:H7/pGFP strain 72 selected in this study was obtained from the USDA (Pina Fratamico, USDA-ARS-ERRC, Wyndmoor, PA). Details on bacterial growth and preparation methods are presented in the Supporting Information (SI).

Bacterial cell size, shape, electrophoretic mobility, surface charge density, hydrophobicity, EPS composition and content were evaluated as a function of ionic strength (IS) (0.1, 1, 10, and 100 mM KCl). The experimental details for the cell characterization are provided in the SI.

Clay Minerals Selection and Characterization. Well crystallized kaolinite (KGa-1b) and montmorillonite (STx-1b) were supplied from the Clay Minerals Society (CMS), Source Clays Repository (University of Purdue, West Lafayette). No pretreatment was done to preserve their natural features and size distribution. Montmorillonite (STx-1b) is a 2:1 (one Al-octahedral sheet sandwiched between two Si-tetrahedral sheets) expanding clay mineral characterized by specific surface area (SSA) of about 83.8 m^2/g and cation exchange capacity (CEC) of 8.4 meq/kg.[33] Kaolinite (KGa-1b) is a 1:1 (one Al-octahedral sheet bonded to one Si-tetrahedral sheet by shared oxygen atoms of the tetrahedral sheet) nonexpanding clay characterized by SSA of 10.1 m^2/g and CEC of 0.2 meq/kg.[34] Goethite was synthesized by the simultaneous addition of a 0.15 M $Fe(NO_3)_3$ solution with the neutralizing 2.5 M KOH in a high-density polyethylene bottle according to the method of Atkinson et al.[35] The SSA and CEC of the goethite were previously measured at 101.6 m^2/g and 0.04 meq/kg.[36] Potentiometric titration of montmorillonite, kaolinite, and goethite was conducted to determine the relative acidity of clay mineral surfaces using an autotitrator (798 MPT Titrino, Metrohm, Switzerland).[37] Acidity values were 1.0, 0.9, 0.9 meq/g, respectively, for montmorillonite, kaolinite, and goethite and corresponding surface charge density (SCD) values were 118.9, 849.7, and 83.2 $\mu C/cm^2$. The size of the minerals was also measured by dynamic light scatting (DLS, Brookhaven Instruments Corporation, Holtsville, NY). The average diameter of montmorillonite, kaolinite, and goethite at 1 mM

KCl was determined to be 2.8 ± 0.3 μm, 3.2 ± 0.1 μm, and 0.6 ± 0.01 μm, respectively. These values fall within the range of diameters reported in the literature for these minerals.[26]

Coating Clay Minerals on Glass Slides. Montmorillonite, kaolinite, or goethite particles were attached to Fisher microscope glass slides (9 mm wide, 20 mm long, and 1.5 mm thick). These slides were used as the collector surfaces in the parallel plate flow system. Polyvinyl alcohol (PVA) (molecular weight of 100 kg/mol) was used as a cementing agent to coat the clay onto the glass slides. The effect of PVA on the mineral surface charge will be discussed later in this paper. Prior to coating, glass slides were cleaned thoroughly and the procedures are presented in the SI. The coating method was a modified form of one previously described[38] wherein clay minerals and PVA were added in 25 mL of deionized (DI) water and their final concentrations were 10 and 0.02 mg/mL, respectively. The ratio of mass concentration between clay and PVA was 500:1. The mixture was vortexed (AutoTouch Mixer model 231, Fisher Scientific) for 5 min and then the glass slides were submerged in the suspension. After 12 h, the coated glass slides were transferred to a glass beaker and dried at room temperature. Excess clay and PVA were removed by repeated washing with DI water followed by drying at room temperature.

Surfaces Characterization of Clay Minerals on Glass Slides. Scanning electron microscope (SEM) micrographs of the clay-coated glass slides were obtained on a Philips XL30-FEG scanning electron microscope operated at 20 kV for each type of clay minerals coating sample. An Au/Pd coating was applied to the samples by sputtering for 90 s prior to taking the image.

To test whether PVA affects the properties of clay minerals in the processes of coating, the hydrophobicity and electrophoretic mobility (EPM) of individual clay minerals and their PVA−mixture were determined. The contact angle of minerals-only, PVA-only, and minerals−PVA mixtures coated on glass slides were determined using a contact angle meter (VCA Optima, AST Products, Inc., Billerica, MA, USA). A total of 12 measurements were made on each sample. The data are reported as an average with the standard deviation for each substrate in Table S1.

The electrophoretic mobility (EPM) of suspended clay minerals without and with PVA ($C_{mineral}/C_{PVA}$ = 500:1) was evaluated at 25 °C and pH 6.0 as a function of IS using a ZetaPALS analyzer (Brookhaven Instruments Corporation, Holtsville, NY). The zeta potential of the samples was calculated from the EPM using the Smoluchowski equation.[39] The results are supplied in Table S1.

DLVO Calculations. DLVO (Derjaguin−Landau−Verwey−Overbeek) theory was applied to calculate the interaction energy between *E. coli* O157:H7 and the clay-coated surfaces.[40,41] Details regarding the total interaction energy calculations are given in the SI.

***E. coli* O157:H7 Deposition and Adsorption Studies.** *E. coli* O157:H7 deposition experiments were conducted in a parallel plate flow chamber (product 31-010, GlycoTech, Rockville, MA) installed on the stage of an upright fluorescence microscope BX-51 (Olympus, Tokyo, Japan), which has been described previously.[42] Briefly, the flow cell is rectangular shaped with an inner chamber 6 cm × 1 cm × 0.0762 cm in size, formed by a Plexiglas block, a flexible silicon elastomer gasket, and a microscope glass slide. The samples (coated glass slides) are inserted in the center of a cast acrylic flow deck. Fluorescently labeled *E. coli* O157:H7 depositing on the surface was imaged by a 40× objective (Olympus UPlanF1, NA, 0.75) focused on the inner surface of the center of the sample using a fluorescent filter set with an excitation wavelength of 480 nm and emission wavelength of 510 nm (Chroma Technology Corp., Brattleboro, VT).

Deposition of bacteria was recorded with a digital camera (Retiga EXI 1394, Qimaging, British Columbia) acquiring images every 30 s for 30 min and analyzed with the supplied software (SimplePCI, Precision Instruments, Inc., Minneapolis, MN). The number of deposited cells was determined for each time interval by comparing the changes between successive images. Injection concentration of bacteria was 1×10^8 cells/mL. A flow rate of 0.1 mL/min was employed, corresponding to an average flow velocity of 0.79 m/h. The value simulates a typical rate in groundwater environments.[42,43] Bacterial deposition experiments were conducted at IS conditions of 0.1, 1, 10, and 100 mM KCl solution at pH 6.0 (adjusted using 10 mM HCl and 10 mM KOH as needed) and ambient temperature (22−25 °C).

The deposition flux (J) was calculated by dividing the initial slope of cells depositing versus time by the microscope viewing area (230 μm × 170 μm). The experimental bacteria transfer rate coefficient, $k_{experiment}$, which is a measure of the deposition kinetics of bacteria, was determined using $k_{experiment} = J/C_0$, where C_0 is injected bacteria concentration.[39]

Adsorption of *E. coli* O157:H7 on clay minerals was also conducted in batch systems using a previously developed method.[13] Bacterial adsorption experiments were conducted at IS conditions of 1, 10, and 100 mM KCl solution at pH 6.0 (adjusted using 10 mM HCl and 10 mM KOH as needed) and ambient temperature (22−25 °C). Further experimental details are given in the SI.

Theoretical Calculation of *E. coli* O157:H7 Transfer Rate Coefficients. Smoluchowski−Levich (SL) approximation of the two-dimensional convective-diffusion equation was used (neglecting surface interactions, hydrodynamic, and external forces) to predict the mass transport in a parallel plate system.[44] In the SL approximation, it is assumed that the substratum surface acts as a perfect sink (i.e., every bacterium that arrives at the surface adheres irreversibly). The SL approximation is based upon the following equation for calculation of a theoretical particle transfer rate coefficient (k_{ideal}):[39,45]

$$k_{ideal} = \frac{D_\infty}{\Gamma\left(\frac{4}{3}\right) a_p}\left(\frac{2Pe}{9x/b}\right)^{1/3} \quad (1)$$

where a_p is bacterial radius, bulk diffusion coefficient (D_∞) is equal to $k_B T/(6\pi\mu a_P)$, the Peclet number (Pe) is equal to $3ua_p^3/(2b^2D)$, k_B is Boltzmann's constant, T is the absolute temperature, u and μ are the fluid velocity and fluid dynamic viscosity, respectively, the gamma function $\Gamma(4/3)$ is equal to 0.893, x is equal to half of the flow chamber length, and b is midway depth of the parallel plate channel.

Survival of *E. coli* O157:H7 on Clay-Coated Surfaces. Survival experiments were conducted utilizing methods developed by Asadishad et al.[32] Briefly, after conducting deposition experiments in the flow chamber with bacteria suspended in 10 mM KCl, a bacteria-free KCl was injected (0.1 mL/min, 10 min) to rinse away any unattached cells. Attached bacteria were stained by filling the chamber with a dye solution consisting of 40 μL Live/Dead BacLight stain (L-7012,

Table 1. Characterization of *E. coli* O157:H7 as a Function of Ionic Strength

IS (mM)	radius (μm)	acidity (10^{-5}mequiv/10^8 cells)	surface charge density (μC/cm^2)	MATH (%)	sugar concentration (mg/10^{10} cells)	protein content (mg/10^{10} cells)	zeta potential (mV)
0.1	0.7 ± 0.01			35.1 ± 2.4			−9.6 ± 1.0
1	0.7 ± 0.01			40.1 ± 5.2			−3.2 ± 2.2
10	0.7 ± 0.01	3.3 ± 0.7	555.9 ± 46.4	36.1 ± 3.2	2.0 ± 0.8	77.6 ± 17.0	−1.8 ± 0.9
100	0.7 ± 0.01			22.6 ± 4.7			−1.4 ± 1.9

Molecular Probes, Eugene, OR) in 2 mL of 10 mM KCl for 15 min. Cells were counted on an hourly basis for 6 h. To prevent photobleaching of the stain, the entire experimental setup was protected from light and the exposure time was minimized. Stained bacteria were imaged by fluorescence microscopy (IX-70, Olympus) using a red/green fluorescence filter set (Chroma Technology Corp., Brattlebora, VT). The BacLight stain was not rinsed from the flow chamber for the entire duration of each experiment. Planktonic cells survival experiments were also evaluated using the same method. The viability is reported as the percentage of viable cells. Each experiment was performed in triplicate on different days.

The viability of cells adhered to minerals was evaluated in this study using Live/Dead BacLight Bacterial Viability Kits, which have been widely used to enumerate viable bacteria. This kit includes SYTO-9 green-fluorescent nucleic acid stain and the red-fluorescent nucleic acid stain propidium iodide. These stains differ both in their spectral characteristics and in their ability to penetrate healthy bacterial cells.[46] The SYTO-9 stain generally labels all bacteria (those with intact membranes and those with damaged membranes), whereas propidium iodide penetrates only bacteria with damaged membranes. With a mixture of the SYTO-9 and propidium iodide stains, bacteria with intact cell membranes stain fluorescent green (considered to be viable), whereas bacteria with damaged membranes stain fluorescent red (considered to be dead).[32,46]

Statistical Analysis. All experiments were performed in triplicate. The data are presented as the mean ± SEM (standard error of the mean). Statistical differences between mean values were analyzed using a Student *t*-test. *P* values greater than or equal to 0.05 suggest differences are statistically insignificant within a 95% confidence interval.

RESULTS AND DISCUSSION

Characteristics of Clay Minerals and *E. coli* O157:H7 Cells. The properties of pure clay minerals and PVA−clay coatings were investigated by water contact angle and zeta potential measurements. These results and the related discussion are provided in the Supporting Information. Cell characteristics of *E. coli* O157:H7 as a function of ionic strength (IS) are presented in Table 1. The equivalent radii of *E. coli* O157:H7 is 0.7 μm, regardless of IS. The measured value of acidity at 10 mM is 3.3×10^{-5} mequiv/10^8 cells, and from this value the surface charge density was calculated as 555.9 μC/cm^2. The titrated surface charge density for *E. coli* O157:H7 tested in this study compares well to the value reported for *E. coli* D21g harvested at midexponential stage (796.8 μC/cm^2).[47] EPS analysis reveals that the content of protein is 38 times higher than that of sugar. This is similar to trends for other *E. coli* in the literature.[8,10,48] MATH test results show no significant difference for the hydrophobicity of bacteria at 0.1, 1, and 10 mM KCl. However, bacterial hydrophobicity decreases significantly at 100 mM KCl. The zeta potentials of bacteria are negative across the range of IS, although there is a general reduction trend with increasing IS. The zeta potentials of *E. coli* O157:H7 have no statistical difference in the range of 1−100 mM KCl and bacterial surfaces appear to be near neutral ($P > 0.05$).

Deposition and Adsorption Behavior of *E. coli* O157:H7. The deposition trends for *E. coli* O157:H7 on montmorillonite, kaolinite, and goethite as a function of IS are shown in Figure 1. Deposition rates ($k_{experiment}$) of negatively

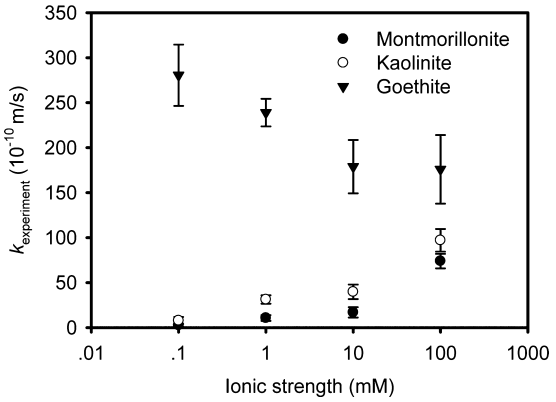

Figure 1. *E. coli* O157:H7 transfer rate coefficients ($k_{experiment}$) as a function of IS as observed in the PP flow chamber.

charged *E. coli* O157:H7 on the positively charged goethite decreased from 280.5×10^{-10} m/s to 175.9×10^{-10} m/s with increasing IS (0.1 to 100 mM, respectively). This trend can be explained by classic DLVO theory.[40,41] The substantial deposition at lower IS is attributed to the presence of an attractive energy well at larger separation distance.[49,50] DLVO interaction profiles were generated (see Figure S1c) and clearly show that the separation distance at which *E. coli* O157:H7 starts to experience attractive force decreases with increasing IS, which was consistent with the observed reduction in $k_{experiment}$ values with greater IS. Additionally, Figure S1 displays a trend that no repulsive force was present between *E. coli* O157:H7 and goethite, demonstrating chemically favorable conditions for *E. coli* O157:H7 interaction with and deposition on goethite surfaces.

The $k_{experiment}$ values for *E. coli* O157:H7 on negatively charged montmorillonite and kaolinite increased with IS. The increase of $k_{experiment}$ with IS for both clay minerals generally agreed with DLVO theory. As shown in Figure S1, montmorillonite and kaolinite had similar energy barriers for *E. coli* O157:H7 which decreased from ∼130 kT at 0.1 mM KCl to ∼12 kT at 1 mM KCl. No energy barrier exists above 1 mM KCl. The increase of solution IS led to the compression of the electrostatic double layer between the clay and cells; as a result, greater deposition efficiencies of *E. coli* O157:H7 were obtained at higher IS.

The adsorption isotherms generated for *E. coli* O157:H7 on montmorillonite, kaolinite, and goethite as a function of IS in

batch systems are shown in Figure S2. The number of cells adsorbed increased with the initial bacterial concentration. The results of these batch experiments were fit by a linear equation which can be described as $C_s = K_d C_{eq}$, where C_s is the amount of cells adsorbed per unit mass of minerals, C_{eq} is the aqueous equilibrium concentration of cells, and K_d is the distribution coefficient. The higher the K_d values, the greater the adsorption capacity of bacteria on minerals. As presented in Table S2, the K_d values of *E. coli* O157:H7 on montmorillonite and kaolinite increased with IS from 1 to 100 mM, while on goethite the distribution coefficient decreased. At the same IS, the K_d values of *E. coli* O157:H7 on minerals were in the sequence of goethite > kaolinite > montmorillonite.

Mechanisms of Bacterial−Clay Interactions. The general cell adhesion trends in batch system were similar to those under flow (Figure S3), confirming that interfacial physicochemical interactions between *E. coli* O157:H7 and clay minerals are responsible for the extent of bacterial deposition under the dynamic conditions of this study. For example, $k_{experiment}$ on kaolinite at 1 and 10 mM was significantly greater than that on montmorillonite ($P < 0.05$). This was despite the zeta potential of kaolinite being significantly more negative than montmorillonite. Similarly, K_d values on montmorillonite were lower than kaolinite in the batch system (Table S2 and Figure S3).

The greater deposition on kaolinite than on montmorillonite was ascribed to chemical heterogeneity of clay minerals which have anisotropic properties in their basal planes surfaces and edge surfaces.[51] Kaolinite (1:1 layer-type) consists of one tetrahedral sheet and one octahedral sheet. The silica tetrahedra of kaolinite carries a small amount of permanent negative charges due to isomorphous substitution of Al^{3+} for Si^{4+}, whereas octahedral and the edge surfaces carry positive or negative charges depending on the pH of the system.[51,52] Montmorillonite (2:1 layer-type) consists of an octahedral sheet sandwiched between two tetrahedral sheets, which has a high amount of negatively permanent layer charges and negligible variable charges.[51,53] The silica face was found to be negatively charged at pH > 4, whereas the alumina face surface was found to be positively charged at pH < 6 and negatively charged at pH > 8.[54] Therefore, at these experimental conditions (pH 6), the two basal planes of montmorillonite were negatively charged, and the octahedral and edge surfaces of kaolinite were positively charged. SEM images showed that kaolinite particles aggregate in the form of face−face and edge−face contacts on glass slides (Figure 2b). Similar phenomena were also observed in other studies.[55,56] Therefore, positive charges from the exposed edge surfaces of kaolinite would attract *E. coli* O157:H7 to deposition on the kaolinite surface, more so than the montmorillonite which has a greater amount of the negatively charged surface area exposed.

Further insight can also be gained when considering that bacterial attachment is controlled by cell transport from the bulk solution to the collector surface and the subsequent interactions between the cell and collector surface occurring upon close approach. The calculated k_{ideal} is 109×10^{-10} m/s, which is approximately 0.6−1.5 times lower than the experimentally determined value for *E. coli* O157:H7 deposition on goethite (favorable conditions) and approximately 0.1−40 times higher than those on montmorillonite and kaolinte (unfavorable conditions). This suggests that electrostatic forces play an important role in *E. coli* O157:H7−clay interactions, and enhance or hinder the resulting deposition on the clay. In addition to attractive long-range electrostatic forces, the higher $k_{experiment}$ of bacteria on goethite compared to k_{ideal} is also probably due to short-range bonding interactions such as hydrogen bond and inner-sphere complexation. Parikh and Chorover[16] used ATR-FTIR spectra to clearly show *Shewanella oneidensis*, *Pseudomonas aeruginosa*, and *Bacillus subtilis* cells attachment to hematite (α-Fe_2O_3) films involves the formation of inner-sphere P−OFe bonds. Using the same technique, Rong et al.[15] also demonstrated that hydrogen bonding is involved in *Pseudomonas putida* adsorption to goethite. It is likely these same types of interactions are contributing to the cell−clay interactions in this study as well. It is worth noting

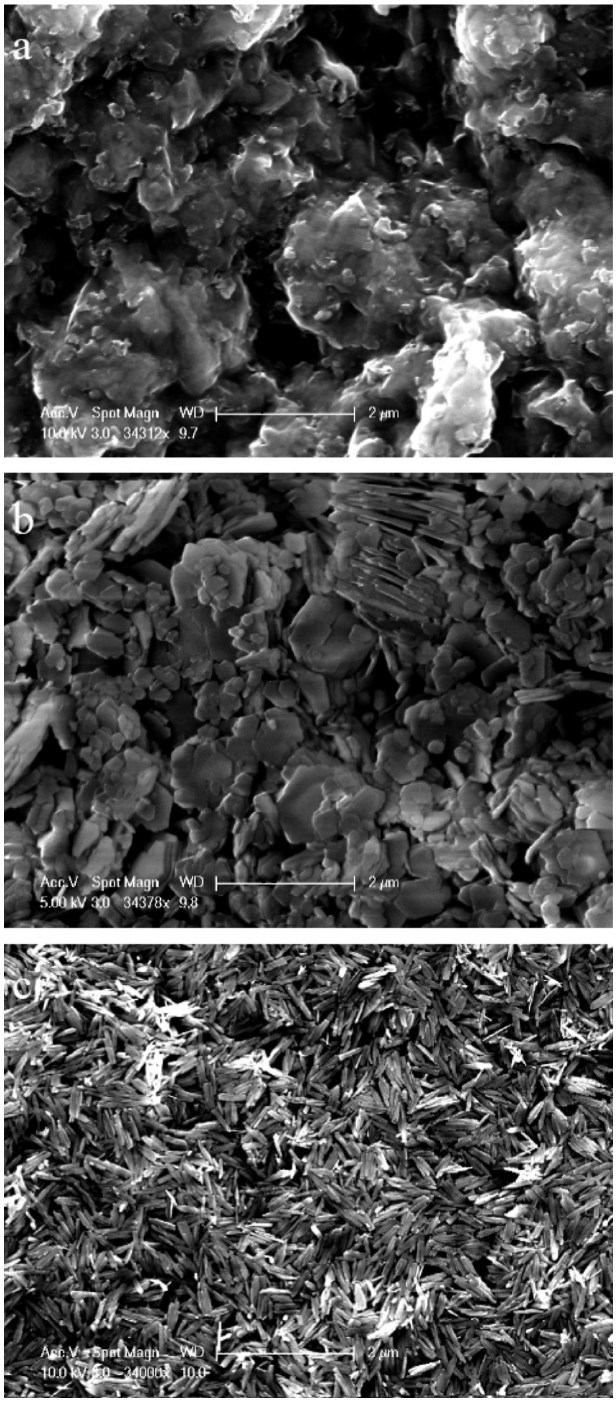

Figure 2. SEM images of (a) montmorillonite, (b) kaolinite, and (c) goethite coated on glass slides.

that interaction mechanisms between bacteria and clay will vary with pH, either due to a change in protonation or inner-sphere complexation to goethite surface sites as pH is modified.[17]

Survival of Attached *E. coli* O157:H7. Figure 3 shows the viability of *E. coli* O157:H7 in the planktonic state and attached

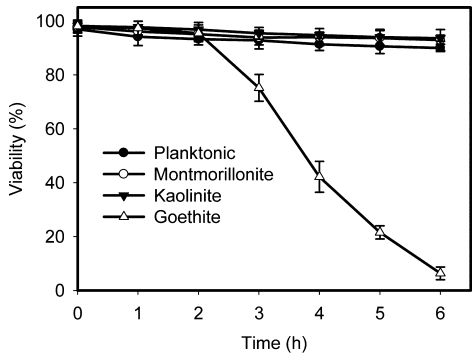

Figure 3. Viability of planktonic and attached bacteria on montmorillonite, kaolinite, and goethite as a function of time.

to montmorillonite, kaolinite, and goethite as a function of time. Suspended and attached cells on montmorillonite and kaolinite remained mostly viable (viability >90%) over a period of 6 h. The viability of attached cells on goethite was initially ~98% (<2 h) and then dropped dramatically to about 6% after 6 h. These results suggest that *E. coli* O157:H7 retains its viability in suspension and when attached to negatively charged clay minerals (montmorillonite and kaolinite); however, interactions with the positively charged goethite were detrimental.

A variety of chemical and physical processes have been proposed to explain the observed loss in activity or viability of bacteria following interaction with clay minerals. Wong et al.[57] reported that kaolinite and bentonite inhibited sulfate-reducing activity in washed *Desulfovibrio vulgaris* suspensions by 62% and 61%, suggesting inhibition is influenced by the released aluminum ion from clays. Recently, Williams et al.[58] demonstrated that the antibacterial mechanism of clay is Fe^{2+} released from clay into the suspension and overwhelms outer membrane regulatory proteins. The iron is oxidized when entering the cell and causes the precipitation of Fe^{3+} and production of lethal hydroxyl radicals. The authors also deduced that extracellular physical processes do not cause cell death.[59] Unlike these two aforementioned studies, ion leaching from the clay was negligible and not the cause of viability loss in this study.

Another potential mechanism that could be occurring is loss of membrane structural integrity from interactions between *E. coli* O157:H7 and clays. Terada et al.[60] investigated the effect of material surface charge property on *E. coli* adhesion and survival, and found that electrostatic attraction forces induced more bacterial retention and lower viability. Other studies have also reported that positively charged biomaterial surfaces exert an antimicrobial effect on adhering bacteria, while negatively charged surfaces have no significant effects on bacterial viability or metabolic activity.[29−32] In this study, positively charged goethite can attract bacteria through long-range electrostatic forces, while negatively charged montmorillonite and kaolinite repulse bacteria (Figure S1). Therefore, the stronger and closer association between bacteria and goethite is responsible for lower bacterial viability as compared to cells bound to montmorillonite and kaolinite. Additionally, the SEM image of goethite showed that it is needle-shaped (Figure 2c), which can possibly pierce into the cell membrane under strong electrostatic attraction forces between goethite and bacteria causing cell death. Using transmission electron microscopy, Glasauer et al.[61] also confirmed the close association between *Shewanella putrefaciens* and Fe(hydr)oxides (ferrihydrite, goethite, and hematite) and suggested that in some instances, the mineral crystals had even penetrated the outer membrane and peptidoglycan layers. Using microcalorimetric techniques, Rong et al.[62] reported goethite can significantly depress the sporulation and the total metabolic activity of *Bacillus thuringiensis*. Their results were explained by the tight binding of goethite on *B. thuringiensis* which may hamper the uptake of essential nutrients, and/or impair efflux of metabolites.[63] However, it is worth mentioning that in these studies the bacteria, clay, and nutrient media were mixed together to cultivate the cells. Due to the complex interfacial interactions among these three, it is hard to ascertain the direct effect of the clay on bacterial activity or viability. In this current study utilizing a flow chamber and batch systems, the effects of attachment to clay minerals surfaces on bacterial viability can be directly determined.

Environmental Implications. Many types of livestock such as cattle, pigs, sheep, and poultry,[64] as well as wildlife including white-tailed deer[65] and feral pigs,[66] are considered a reservoir of *E. coli* O157:H7. For domesticated animals, their manure produced in the farms is commonly applied to agricultural fields as a fertilizer. Wildlife feces are also distributed in uncontrolled ways. Therefore, *E. coli* O157:H7 cells are introduced into the soil through these processes. Findings from this study suggest soils containing goethite (e.g., Ultisols and Oxisols) have greater adhesion capacity for *E. coli* O157:H7 and the interactions are detrimental to pathogens. Other types of soils (Alfisols) having montmorillonite and kaolinite may show less retention of such a bacterial pathogen; however, they may be a more favorable environment for pathogen survival. The results presented herein demonstrate the dominating role both chemical (e.g., surface charge) and physical (e.g., morphology and roughness) properties of clays may have on bacterial pathogen deposition and survival. They also provide insight into the interaction mechanisms between bacteria and clays, which is vital to understand and predict microbial soil quality. Future confirmation of these results using other types of bacteria and environmental conditions (e.g., pH, humic acid, temperature) is merited.

■ ASSOCIATED CONTENT

Supporting Information

(1) Additional details on the materials and methods; (2) additional details on the results and discussion; (3) a table showing water contact angles of PVA, clay minerals, and their mixtures on glass slides; (4) a table of fitted parameters for *E. coli* O157:H7 adsorption on clay minerals as a function of IS at pH 6.0; (5) a figure of calculated DLVO interaction energies between *E. coli* O157:H7 and the three model clays as a function of separation distance and IS; (6) equilibrium adsorption data (isotherms) of *E. coli* O157:H7 on the three model clays as a function of IS; and finally, (7) a figure of comparison between $k_{experiment}$ in the parallel plate flow system and K_d in the batch system at different concentrations of KCl. This material is available free of charge via the Internet at http://pubs.acs.org.

AUTHOR INFORMATION

Corresponding Author

*E-mail: swalker@engr.ucr.edu; tel: (951)827-6094; fax: (951) 827-5696.

Notes

The authors declare no competing financial interest.

ACKNOWLEDGMENTS

This work was supported by the National Natural Science Foundation of China (41171196, 40825002) and the Foundation for the Author of National Excellent Doctoral Dissertation of China (201066).

REFERENCES

(1) Boyce, T. G.; Swerdlow, D. L.; Griffin, P. M. *Escherichia coli* O157:H7 and the hemolytic-uremic syndrome. *N. Engl. J. Med.* **1995**, *333*, 364−368.

(2) Mead, P. S.; Slutsker, L.; Dietz, V.; McCaig, L. F.; Bresee, J. S.; Shapiro, C.; Griffin, P. M.; Tauxe, R. V. Food-related illness and death in the United States. *Emerging Infect. Dis.* **1999**, *5*, 607−625.

(3) Cieslak, P. R.; Barrett, T. J.; Griffin, P. M.; Gensheimer, K. F.; Beckett, G.; Buffington, J.; Smith, M. G. *Escherichia coli* O157:H7 infection from a manured garden. *Lancet* **1993**, *342*, 367−371.

(4) Armstrong, G. L.; Hollingsworth, J.; Morris, J. G. Emerging foodborne pathogens: *Escherichia coli* O157:H7 as a model of entry of a new pathogen into the food supply of the developed world. *Epidemiol. Rev.* **1996**, *18*, 29−51.

(5) Morrow, I. B.; Stration, R.; Yang, H.-H.; Smets, B. F.; Grasso, D. Macro- and nanoscale observations of adhesive behavior for several *E. coli* strains (O157:H7 and environmental isolates) on mineral surfaces. *Environ. Sci. Technol.* **2005**, *39*, 6395−6404.

(6) Bradford, S. A.; Simunek, J.; Walker, S. L. Transport and straining of *E coli* O157: H7 in saturated porous media. *Water Resour. Res.* **2006**, *42*, W12S12.

(7) Castro, F. D.; Tufenkji, N. Relevance of nontoxigenic strains as surrogates for *Escherichia coli* O157: H7 in groundwater contamination potential: Role of temperature and cell acclimation time. *Environ. Sci. Technol.* **2007**, *41*, 4332−4338.

(8) Haznedaroglu, B. Z.; Kim, H. N.; Bradford, S. A.; Walker, S. L. Relative transport behavior of *Escherichia coli* O157:H7 and *Salmonella enterica* Serovar Pullorum in packed bed column systems: Influence of solution chemistry and cell concentration. *Environ. Sci. Technol.* **2009**, *43*, 1838−1844.

(9) Kim, H. N.; Bradford, S. A.; Walker, S. L. *Escherichia coli* O157: H7 transport in saturated porous media: Role of solution chemistry and surface macromolecules. *Environ. Sci. Technol.* **2009**, *43*, 4340−4347.

(10) Kim, H. N.; Hong, Y. S.; Lee, I.; Bradford, S. A.; Walker, S. L. Surface characteristics and adhesion behavior of *Escherichia coli* O157: H7: Role of extracellular macromolecules. *Biomacromolecules* **2009**, *10*, 2556−2564.

(11) Wang, L. X.; Xu, S. P.; Li, J. Effects of phosphate on the transport of *Escherichia coli* O157: H7 in saturated quartz sand. *Environ. Sci. Technol.* **2011**, *45*, 9566−9573.

(12) Schinner, T.; et al. Transport of selected bacterial pathogens in agricultural soil and quartz sand. *Water Res.* **2010**, *44*, 1182−1192.

(13) Jiang, D. H.; Huang, Q. Y.; Cai, P.; Rong, X. M.; Chen, W. L. Adsorption of *Pseudomonas putida* on clay minerals and iron oxide. *Colloids Surf. B* **2007**, *54*, 217−221.

(14) Rong, X. M.; Huang, Q. Y.; He, X. M.; Chen, H.; Cai, P.; Liang, W. Interaction of *Pseudomonas putida* with kaolinite and montmorillonite: A combination study by equilibrium adsorption, ITC, SEM and FTIR. *Colloids Surf. B* **2008**, *64*, 49−55.

(15) Rong, X. M.; Chen, W. L.; Huang, Q. Y.; Cai, P.; Liang, W. *Pseudomonas putida* adhesion to goethite: Studied by equilibrium adsorption, SEM, FTIR and ITC. *Colloids Surf. B* **2010**, *80*, 79−85.

(16) Parikh, S. J.; Chorover, J. ATR-FTIR spectroscopy reveals bond formation during bacterial adhesion to iron oxide. *Langmuir* **2006**, *22*, 8492−8500.

(17) Elzinga, E. J.; Huang, J. H.; Chorover, J.; Kretzschmar, R. ATR-FTIR spectroscopy study of the influence of pH and contact time on the adhesion of *Shewanella putrefaciens* bacterial cells to the surface of hematite. *Environ. Sci. Technol.* **2012**, *46*, 12848−12855.

(18) Fang, L. C.; Cao, Y. Y.; Huang, Q. Y.; Walker, S. L.; Cai, P. Reactions between bacterial exopolymers and goethite: A combined macroscopic and spectroscopic investigation. *Water Res.* **2012**, *46*, 5613−5620.

(19) Hong, Z. N.; Rong, X. M.; Cai, P.; Liang, W.; Huang, Q. Y. Effects of temperature, pH and salt concentrations on the adsorption of *Bacillus subtilis* on soil clay minerals investigated by microcalorimetry. *Geomicrobiol. J.* **2011**, *28*, 686−691.

(20) Wang, G.; Zhao, T.; Doyle, M. P. Fate of enterohemorrhagic *Escherichia coli* O157:H7 in bovine feces. *Appl. Environ. Microbiol.* **1996**, *62*, 2567−2570.

(21) Kudva, I. T.; Blanch, K.; Hovde, C. J. Analysis of *Escherichia coli* O157:H7 survival in ovine or bovine manure and manure slurry. *Appl. Environ. Microbiol.* **1998**, *64*, 3166−3174.

(22) Himathongkham, S.; Bahari, S.; Riemann, H.; Cliver, D. Survival of *Escherichia coli* O157:H7 and *Salmonella Typhimurium* in cow manure and cow manure slurry. *FEMS Microbiol. Lett.* **1999**, *178*, 251−257.

(23) Jiang, X. P.; Morgan, J.; Doyle, M. P. Fate of *Escherichia coli* O157:H7 in manure-amended soil. *Appl. Environ. Microbiol.* **2002**, *68*, 2605−2609.

(24) Coroller, L.; Leguerinel, I.; Mettler, E.; Savy, N.; Mafart, P. General model, based on two mixed Weibull distributions of bacterial resistance, for describing various shapes of inactivation curves. *Appl. Environ. Microbiol.* **2006**, *72*, 6439−6502.

(25) Ma, J. C.; Ibekwe, A. M.; Yi, X.; Wang, H. Z.; Yamazaki, A.; Crowley, D. E.; Yang, C. H. Persistence of *Escherichia coli* O157:H7 and its mutants in soils. *PLOS One* **2011**, *6*, e23191.

(26) Sumner, M. E. *Handbook of Soil Science*; CRC Press: Boca Raton, FL, 2000.

(27) Semenov, A. V.; van Overbeek, L.; van Bruggen, A. H. C. Percolation and survival of *Escherichia coli* O157:H7 and *Salmonella enterica* serovar Typhimurium in soil amended with contaminated dairy manure or slurry. *Appl. Environ. Microbiol.* **2009**, *75*, 3206−3205.

(28) Avery, L. M.; Williams, A. P.; Killham, K.; Jones, D. L. Survival of *Escherichia coli* O157:H7 in waters from lakes, rivers, puddles and animal drinking troughs. *Sci. Total Environ.* **2008**, *389*, 378−385.

(29) Weiger, R.; Decker, E. M.; Krastl, G.; Brecx, M. Deposition and retention of vital and dead *Streptococcus sanguinis* cells on glass surfaces in a flow-chamber system. *Arch. Oral Biol.* **1999**, *44*, 621−628.

(30) Ven der Mei, H. C.; Rustema-Abbing, M.; Langworthy, D. E.; Collias, D. I.; Mitchell, M. D.; Bjorkquist, D. W.; Busscher, H. J. Adhesion and viability of waterborne pathogens on p-DADMAC coatings. *Biotechnol. Bioeng.* **2008**, *99*, 165−169.

(31) Ven der Mei, H. C.; Atema-Smit, J.; Jager, D.; Langworthy, D. E.; Collias, D. I.; Mitchell, M. D.; Busscher, H. J. Influence of adhesion to activated carbon particles on the viability of waterborne pathogenic bacteria under flow. *Biotechnol. Bioeng.* **2008**, *100*, 810−813.

(32) Asadishad, B.; Ghoshal, S.; Tufenkji, N. Method for the direct observation and quantification of survival of bacteria attached to negatively or positively charged surfaces in an aqueous medium. *Environ. Sci. Technol.* **2011**, *45*, 8345−8351.

(33) Van Olphen, H.; Fripiat, J. J. *Data Handbook for Clay Minerals and Other Non-Metallic Materials*; Pergamon Press, 1979.

(34) Pruett, R. J.; Webb, H. L. Sampling and analysis of KGa-1B well-crystallized kaolin source clay. *Clay Clay Miner.* **1993**, *41*, 514−519.

(35) Atkinson, R. J.; Posner, A. M.; Quirk, J. P. Adsorption of Potential Determining Ions at the Ferric Oxide Aqueous Electrolyte Interface. *J. Phys. Chem.* **1967**, *71*, 550−558.

(36) Cai, P.; Huang, Q. Y.; Zhang, X. W. Microcalorimetric studies of the effects of $MgCl_2$ concentrations and pH on the adsorption of DNA

on montmorillonite, kaolinite and goethite. *Appl. Clay Sci.* **2006**, *32*, 147−152.
(37) Fang, L. C.; Huang, Q. Y.; Wei, X.; Rong, X. M.; Chen, W. L.; Cai, P. Microcalorimetric and potentiometric titration studies on the adsorption of copper by extracellular polymeric substances (EPS), minerals and their composites. *Bioresour. Technol.* **2010**, *101*, 5774−5779.
(38) Jerez, J.; Flury, M.; Shang, J. Y.; Deng, Y. J. Coating of silica sand with aluminosilicate clay. *J. Colloid Interface Sci.* **2006**, *294*, 155−164.
(39) Elimelech, M.; Gregory, J.; Jia, X.; Williams, R. A. *Particle Deposition and Aggregation: Measurement, Modeling and Simulation*; Butterworth-Heinemann: Newton, MA, 1995.
(40) Derjagin, B. V.; Landau, L. D. Particle deposition on ideal collectors from dilute flowing suspensions: Mathematical formulation, numerical solution, and simulations. *Acta Physicochim. URSS* **1941**, *14*, 633−662.
(41) Verwey, E. J. W.; Overbeek, J. T. G. *Theory of the Stability of Lyophobic Colloids: The Interaction of Sol Particles Having an Electric Double Layer*; Elsevier: Amsterdam, 1948.
(42) Chen, G. X.; Hong, Y. S.; Walker, S. L. Colloidal and Bacterial Deposition: Role of Gravity. *Langmuir* **2010**, *26*, 314−319.
(43) Crittenden, J. C.; Harza, M. W. *Water Treatment Principles and Design*; J. Wiley: Hoboken, NJ, 2005.
(44) Elimelech, M. Particle deposition on ideal collectors from dilute flowing suspensions: Mathematical formulation, numerical solution, and simulations. *Sep. Technol.* **1994**, *4*, 186−212.
(45) Chen, G. X.; Bevig, D. E.; Bedi, R. S.; Yan, Y. S.; Walker, S. L. Initial bacterial deposition on bare and zeolite-coated aluminum alloy and stainless steel. *Langmuir* **2009**, *25*, 1620−1626.
(46) Boulos, L.; Prédvost, M.; Barbeau, B.; Coallier, J.; Desjardins, R. LIVE/DEAD ® BacLight (TM): application of a new rapid staining method for direct enumeration of viable and total bacteria in drinking water. *J. Microbiol. Methods* **1999**, *37*, 77−86.
(47) Walker, S. L.; Redman, J. A.; Elimelech, M. Influence of growth phase on bacterial deposition: Interaction mechanisms in packed-bed column and radial stagnation point flow systems. *Environ. Sci. Technol.* **2005**, *39*, 6405−6411.
(48) Chowdhury, I.; Cwiertny, D. M.; Walker, S. L. Combined factors influencing the aggregation and deposition of nano-TiO_2 in the presence of humic acid and bacteria. *Environ. Sci. Technol.* **2012**, *46*, 6968−6976.
(49) Elimelech, M. Kinetics of capture of colloidal particles in packed beds under attractive colloidal interactions. *J. Colloid Interface Sci.* **1991**, *146*, 337−352.
(50) Fatisson, J.; Domingos, R. F.; Wilkinson, K. J.; Tufenkji, N. Deposition of TiO_2 nanoparticles onto silica measured using a quartz crystal microbalance with dissipation monitoring. *Langmuir* **2009**, *25*, 6062−6069.
(51) Sposito, G. *The Surface Chemistry of Soils*; Oxford University Press: New York, 1984.
(52) Tombácz, E.; Szekeres, M. Surface charge heterogeneity of kaolinite in aqueous suspension in comparison with montmorillonite. *Appl. Clay Sci.* **2006**, *34*, 105−124.
(53) Tombacz, E.; Szekeres, M. Colloidal behavior of aqueous montmorillonite suspensions: The specific role of pH in the presence of indifferent electrolytes. *Appl. Clay Sci.* **2004**, *27*, 75−94.
(54) Gupta, V.; Hampton, M. A.; Stokes, J. R.; Nguyen, A. V.; Miller, J. D. Particle interactions in kaolinite suspensions and corresponding aggregate structures. *J. Colloid Interface Sci.* **2011**, *359*, 95−103.
(55) Wan, J.; Tokunaga, T. K. Partitioning of clay colloids to gas-water interfaces. *J. Colloid Interface Sci.* **2002**, *247*, 54−67.
(56) Gupta, V.; Miller, J. D. Surface force measurements at the basal planes of ordered kaolinite particles. *J. Colloid Interface Sci.* **2010**, *344*, 362−371.
(57) Wong, D.; Suflita, J. M.; Mckinley, J. P.; Krumholz, L. R. Impact of clay minerals on sulfate-reducing activity in aquifers. *Microb. Ecol.* **2004**, *47*, 80−6.
(58) Williams, L. B.; Metge, D. W.; Eberl, D. D.; Harvey, R. W.; Turner, A. G.; Prapaipong, P.; Poret-Peterson, A. T. What makes a natural clay antibacterial? *Environ. Sci. Technol.* **2011**, *45*, 3768−3773.
(59) Williams, L. B.; Haydel, S. E. Evaluation of the medicinal use of clay minerals as antibacterial agents. *Int. Geol. Rev.* **2010**, *52*, 745−770.
(60) Terada, A.; Okuyama, K.; Nishikawa, M.; Tsuneda, S.; Hosomi, M. The effect of surface charge property on *Escherichia coli* initial adhesion and subsequent biofilm formation. *Biotechnol. Bioeng.* **2012**, *109*, 1745−1754.
(61) Glasauer, S.; Langley, S.; Beveridge, T. J. Sorption of Fe (Hydr)Oxides to the surface of *Shewanella putrefaciens*: Cell-bound fine-grained minerals are not always formed de novo. *Appl. Environ. Microbiol.* **2001**, *67*, 5544−5550.
(62) Rong, X. M.; Huang, Q. Y.; Chen, W. L. Microcalorimetric investigation on the metabolic activity of *Bacillus thuringiensis* as influenced by kaolinite, montmorillonite and goethite. *Appl. Clay Sci.* **2007**, *38*, 97−103.
(63) Keen, G. A.; Prosser, J. I. The surface growth and activity of Nitrobacter. *Microb. Ecol.* **1988**, *15*, 21−39.
(64) Chapman, P. A.; Siddons, C. A.; Cerdon-Malo, A. T.; Harkin, M. A. A 1-year study of *Escherichia coli* O157:H7 in cattle, sheep, pigs, and poultry. *Epidemiol. Infect.* **1997**, *119*, 245−250.
(65) Rice, D. H.; Hancock, D. D.; Besser, T. E. Fecal culture of wild animals for *Escherichia coli* O157:H7. *Vet. Rec.* **2003**, *152*, 82−83.
(66) Jay, M. T.; Cooley, M.; Carychao, D.; Wiscomb, G. W.; Sweiter, R. A.; Crawford-Miksza, L.; Asmundson, R. V.; Atwill, E. R.; Mandrell, R. E. *Escherichia coli* O157:H7 in feral swine near spinach fields and cattle, Central California Coast. *Emerg. Infect. Dis.* **2007**, *13*, 1908−1911.